Tumor deformation correction for an image guidance system in breast conserving surgery

Winona L. Richey[1], Jon Heiselman[1], Morgan Ringel[1], Ingrid M. Meszoely[2], Michael I. Miga[1,3,4,5]

[1] *Vanderbilt University, Department of Biomedical Engineering, Nashville, TN USA*
[2] *Vanderbilt University Medical Center, Division of Surgical Oncology, Nashville, TN USA*
[3] *Vanderbilt University Department of Radiology and Radiological Sciences, Nashville, TN USA*
[4] *Vanderbilt Institute for Surgery and Engineering, Nashville, TN USA*
[5] *Vanderbilt University Medical Center, Department of Neurological Surgery, Nashville, TN USA*

ABSTRACT

Breast cancer is the most common cancer in women, and surgical resection is standard of care for the majority of breast cancer patients. Unfortunately, current reoperation rates are 10-29%. Uncertainty in lesion localization is one of the main factors contributing to these high reoperation rates. This work uses the linearized iterative boundary reconstruction approach to model patient breast deformation due to abduction of the ipsilateral arm. A preoperative supine magnetic resonance (MR) image was obtained with the patient's arms down near the torso. A mock intraoperative breast shape was measured from a supine MR image obtained with the patient's arm up near the head. Sparse data was subsampled from the full volumetric image to represent realistic intraoperative data collection: surface fiducial points, the intra-fiducial skin surface, and the chest wall as measured with 7 tracked ultrasound images. The deformed preoperative arm-down data was compared to the ground truth arm-up data. From rigid registration to model correction the tumor centroid distance improves from 7.3 mm to 3.3 mm, average surface fiducial error across 9 synthetic fiducials and the nipple improves from 7.4 ± 2.2 to 1.3 ± 0.7, and average subsurface error across 14 corresponding features improves from 6.2 ± 1.4 mm to 3.5 ± 1.1 mm. Using preoperative supine MR imaging and sparse data in the deformed position, this modeling framework can correct for breast shape changes between imaging and surgery to more accurately predict intraoperative position of the tumor as well as 10 surface fiducials and 14 subsurface features.

Keywords: breast conserving surgery, image-guided surgery, soft tissue deformation, breast cancer, lumpectomy, registration, biomechanical modeling

1. INTRODUCTION

In the United States, over 287,000 people are expected to be diagnosed with breast cancer in 2022[1]. Of these cases, approximately two thirds will undergo breast conserving surgery[2]. Current lesion localization strategies for breast conserving surgery (e.g. radioactive seed, magnetic seed, SAVI Scout) use a seed-based marker or guidewire preoperatively implanted under serial cross-sectional image guidance. While these methods provide valuable subsurface information, they cannot provide full intraoperative tumor boundaries, which are essential to reliably obtain complete resection. This difficulty in localizing tumor boundaries intraoperatively leads to uncertainty in the oncological margin, incomplete resections, and high reoperation rates of 10-29%[3-6].

Magnetic resonance imaging offers high sensitivity for breast cancer[7, 8], and provides improved understanding of intraoperative tumor shape and position when scans are performed in a supine position[9-11]. Several groups have demonstrated the utility of viewing information from supine MR during breast conserving surgery[12-15]. Image-to-physical image guidance platforms that align these high contrast and high-resolution preoperative imaging with the intraoperative patient can predict the full tumor extent in the operating room and assist surgeons with localizing more exact tumor boundaries. However, such image-to-physical guidance platforms to date have utilized rigid registration to describe breast motions between imaging and surgery that are inherently nonrigid. Although there have been indications of growing interest in preoperative supine MR so that imaging more closely aligns with the supine patient presentation in surgery[12-15], significant deformations occur between imaging and surgery even in the context of preoperative supine MR[16]. These image-to-surgical deformations arise due to changes in patient positioning, arm motion, and rotation of the operating room (OR) table. In particular, while supine imaging is performed with the arms down within the closed MR bore, supine operative position places the arm abducted 90 degrees in a T-shape orientation.

Nonrigid deformation-corrected registration methods offer improvement over conventional rigid registration. A method presented by Ebrahimi et al. improved registration error evaluated at the centroid of six tumors from 3–18 mm with rigid registration to 1–10 mm using thin plate splines on surface fiducials[17]. Conley et al. presented a nonrigid finite element method (FEM) correction approach utilizing the chest wall from tracked ultrasound and MR-visible surface fiducials digitized with a stylus, and demonstrated reduction in the centroid errors of two tumors from 6.5 and 12.5 mm after rigid registration to 5.5 and 5.3 mm after correction, respectively[18]. In the method of Conley et al., displacements on the skin surface were estimated via fiducial misalignment after rigid registration. This fiducial misalignment was used in a forward FEM solution approach, with displacements prescribed on the superior and inferior boundaries of the organ. While this approach reduced errors when compared to rigid registration, the true loading on breast tissue is more complex.

In contrast, inverse modeling approaches aim to reconstruct these complex true loading conditions. Given a set of sparse data constraints supplied to the algorithm, the linearized iterative boundary reconstruction (LIBR) method, as presented in Heiselman *et al.*[19], solves for a profile of applied distributed loads that produce the observed intraoperative organ shape. Here the LIBR method is employed to predict breast deformation from abduction of the arm. The framework presented here is tailored to applications in breast conserving surgery, with consideration to the sparse data sources that are amenable to workflow in this intraoperative environment. This work presents this novel deformation correction framework to predict breast shape changes due to arm motion in the supine position.

2. METHODOLOGY

2.1 Patient Data Collection

One 71-year-old breast cancer patient was enrolled with informed consent in this study approved by the Institutional Review Board at Vanderbilt University. The patient had biopsy-confirmed invasive mammary carcinoma in the left breast. Nine MR-visible fiducials were placed on the breast surface. A THRIVE (T_1-weighted, high resolution isotropic volume excitation) sequence with fat suppression was used to obtain supine MR images. A 16-channel sensitivity encoding torso coil (SENSE XL Torso Coil, Philips Healthcare) was placed over the patient's torso and suspended with padding to avoid breast compression. The field of view was 200 mm × 200 mm × 160 mm, centered around the left breast, and the reconstructed voxel size was 0.391 mm × 0.391 mm × 1 mm. The patient was imaged in the supine position with her arm down at her side. This image was used as the preoperative image. The patient's ipsilateral arm was then moved above the head and she was imaged again. This second image was used to obtain mock intraoperative data. In both images the breast tissue was segmented semi-automatically in ITK-Snap and the segmentation was manually

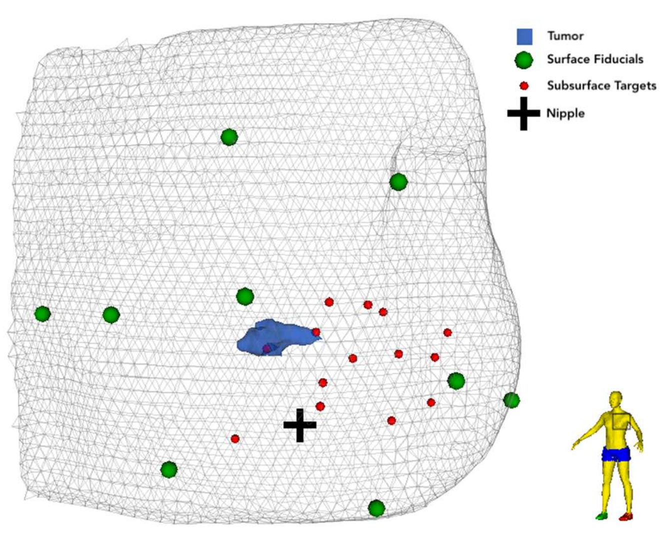

Figure 1: Validation points in the preoperative data designated from a supine MR image, including locations of tumor, surface fiducials, subsurface features (targets) and the nipple (+) on the preoperative breast model.

corrected. Using a custom built software[20], the segmentation was discretized into a 3D mesh of 40,336 tetrahedral elements with edge lengths of 4 mm and a total internal volume of 503 cm^3.

In the preoperative (arm-down) supine MR image, the following features can be designated: surface fiducials, nipple, and the tumor boundary. These data are shown in Figure 1. The segmented tumor volume was 646 mm^3. The roughly ellipsoid shape had a major axis of about 26 mm and both minor axes approximately 10 mm. Additionally, the chest wall and skin surfaces can be designated and subsampled from the breast model boundary.

In the intraoperative (arm-up) supine MR image, the same features are identified. The surface fiducials are identified, and the chest wall and skin surfaces are subsampled from the breast model boundary to mimic feasible intraoperative data collection. The chest wall surface is subsampled to represent chest wall segmentations in seven tracked ultrasound images, and the skin surface is subsampled to only include data within the fiducials (the intra-fiducial surface points). Additionally, 14 subsurface homologous points are identified in both images to be used for validation.

2.2 Registration Method

To correct for nonrigid deformations, the linearized iterative boundary reconstruction (LIBR) method introduced by Heiselman *et al.* [19] is employed. At static equilibrium, linear elasticity is governed by the Navier Cauchy equations,

$$\frac{E}{2(1+\nu)}\nabla^2\boldsymbol{u} + \frac{E}{2(1+\nu)(1-2\nu)}\nabla(\nabla\cdot\boldsymbol{u}) + \boldsymbol{F} = \boldsymbol{0} \tag{1}$$

with E = 2100 Pa as Young's Modulus, ν = 0.45 as Poisson's ratio, $\boldsymbol{u}$ as the displacements, and $\boldsymbol{F}$ as the applied forces. In short, the LIBR method iteratively reconstructs the intraoperative position from a superposed formulation of boundary conditions. A series of control points are distributed on the surface of the organ and every control point is perturbed in each of the three cartesian directions. For each of these perturbations, deformation solutions are pre-computed with a forward solved finite element approach. At runtime the optimal linear combination of these deformation solutions is determined by minimizing the objective function,

$$\Omega(\boldsymbol{\alpha},\boldsymbol{\tau},\boldsymbol{\theta}) = \sum_{F}\frac{\omega_F}{N_F}\sum_{i=1}^{N_F} f_i^{\,2} + \omega_E f_E^{\,2} \tag{2}$$

where f_i represents the distance between an intraoperative data point and the registered preoperative model, f_E represents the strain energy of the deformation, ω_F represents the weight of a feature F, N_F represents the number of points within feature F, and ω_E represents the strain energy weight. The parameters for the objective function are the weight vector $\boldsymbol{\alpha}$ that encodes the deformation state, $\boldsymbol{\tau}$ which represents the rigid translations, and $\boldsymbol{\theta}$ which represents rigid rotations. All features are weighted equally, with ω_F=1.0 m^{-2}, and the strain energy is weighted with ω_E=10^{-9} Pa^{-2}.

Framework feasibility is demonstrated with sparse data that could be realistically obtained in the operating room. The features used to drive the model are the chest wall, the skin surface, and surface fiducials. The chest wall as segmented from the supine MR image is down-sampled to mimic chest wall segmentations in seven ultrasound images with 40 mm width and the skin surface is limited to the intra-fiducial skin nodes. The model-data error, f_i, for each feature is computed based on the type of correspondence, with fiducials treated as corresponding points, and skin and chest wall data treated as point-to-surface correspondences as described in Heiselman *et al.*[19].

The nonrigid model accuracy is compared to two rigid registration approaches: point-based registration using the fiducials, and iterative closest point (ICP) registration of the fully tumor surface. For point-based registration, the preoperative and intraoperative spaces are rigidly registered using 10 corresponding surface points: nine surface fiducials and the nipple. Though ICP registration of full tumor volumes is not feasible intraoperatively, this alignment of the tumor surfaces represents the rigid mismatch in segmentations of the tumor in the two MR images. Note that ICP was performed directly between segmented tumor volumes, not between the outer breast surfaces.

The nonrigid model accuracy is evaluated using differing amounts of intraoperative data. The fiducials, intra-fiducial skin surface, and seven chest-wall segments are used in all three nonrigid correction approaches. In practice, breast cancer patients often have an implanted marker in or near the tumor—either a biopsy clip or a specific localization device such as a magnetic, radioactive, or infrared-reflecting seed. These devices can be localized intraoperatively in tracked ultrasound images. Analysis is therefore extended, including a subsurface feature as additional point-based input to the model. Here, the tumor's nearest neighbor is considered, with the number of included subsurface features k=1. Conversely, when k=0, the model is run as previously described with no subsurface feature points included. Finally, the full tumor surface is included as a point-to-surface correspondence. While this data collection is not feasible intraoperatively, this analysis provides a nonrigid comparator to the rigid ICP alignment, though the nonrigid correction includes a larger distribution of data. No subsurface feature points were included in either of the registration approaches that include the full tumor surface as input to the registration.

2.3 Subsurface Validation: Tumors and Targets

To evaluate model performance, the predicted tumor location was compared with the observed tumor location in the mock-intraoperative image. Boundary nodes of the predicted tumor are evaluated with tumor centroid distance, as well as the modified, maximum, average and $K_{95\%}$ Hausdorff Distances[21]. The DICE coefficient is also reported. Alignment of the homologous subsurface points was compared where target registration error is reported as the average distance between the intraoperative point location, and the model deformed point location.

3. RESULTS

With rigid registration, the tumor centroid distance was 7.3 mm. Average target errors across the 14 corresponding subsurface features, and average fiducial registration errors across the 10 corresponding surface fiducials are displayed in Table 1. As shown in Figure 2, and demonstrated by the 2% DICE coefficient in Table 2, the tumor volumes are largely not overlapping with rigid alignment.

Table 1: Registration error values in millimeters (average ± standard deviation) at surface and subsurface features. Rigid registration methods include iterative closest point (ICP) and point-based. For nonrigid registration methods, k denotes the number of subsurface neighbors included in driving the model.

	Rigid Correction		**Nonrigid Correction**		
	Point-Based	**ICP**	***k*=0**	***k*=1**	**Tumor Surface**
Surface Fiducials	7.4 ± 2.0	10.3 ± 6.7	1.0 ± 0.4	1.3 ± 0.7	1.3 ± 0.7
Subsurface Features	6.2 ± 1.4	4.8 ± 3.5	3.5 ± 1.1	3.3 ± 1.1	3.1 ± 1.4

Table 2: Tumor overlap metrics after registration. Rigid registration methods include iterative closest point (ICP) and point-based. For nonrigid registration methods, k denotes the number of subsurface neighbors included in driving the model.

	Rigid Registration		**Nonrigid Registration**		
	Point-Based	**ICP**	***k*=0**	***k*=1**	**Tumor Surface**
Tumor Centroid Distance (mm)	7.3	0.5	4.4	3.3	2.4
DICE Coefficient	2%	84%	32%	40%	62%
Hausdorff Distance (mm)					
Modified	4.1	0.6	2.3	1.9	1.3
Maximum	9.3	3.1	6.2	4.9	4.4
Average	3.9	0.4	2.0	1.6	1.0
$K_{95\%}$	7.0	1.1	4.4	3.2	2.4

Iterative closest point (ICP) registration provides a high overlap between the two tumor surfaces with a DICE coefficient of 84%, though intraoperative measurement of the full, dense tumor surface is not practical. Importantly, this volume overlap comes at the cost of fiducial and target error. Compared to rigid registration, ICP registration error at the fiducials is *increased* by 39%. Though we see an improvement in target error with the ICP registration, note that the targets are mainly distributed in the same local region as the tumor, as shown in Figure 1.

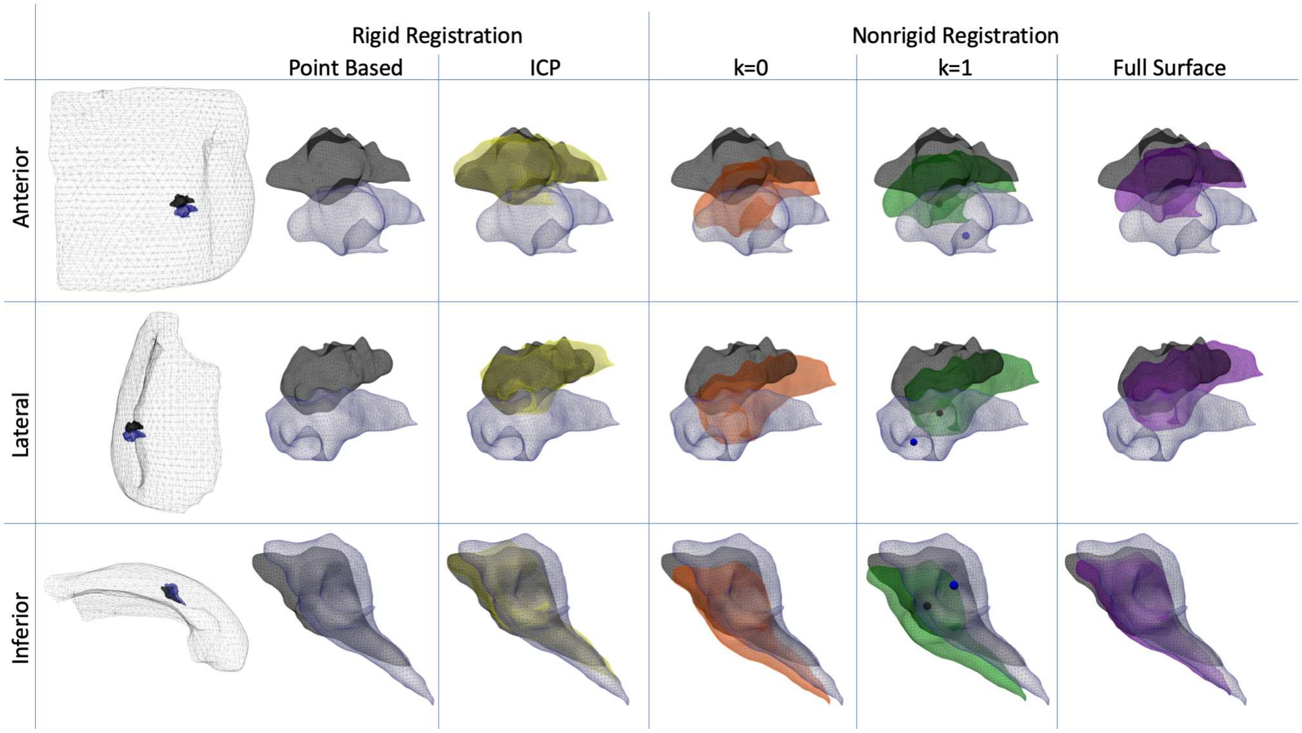

Figure 2: Tumor overlap after registration. Leftmost images show the preoperative breast mesh with preoperative tumor (blue) and ground truth intraoperative tumor position (black) after rigid point-based registration. For *k*=1, the mock biopsy clip position is displayed as a point with the preoperative location in blue and the intraoperative location in black.

With deformation correction and no included subsurface feature points (*k*=0), subsurface feature error becomes 3.5 ± 1.1 mm, providing 44% improvement over rigid registration. Fiducial registration error becomes 1.0 ± 0.4 with deformation correction, providing 86% improvement over rigid correction. At the tumor, point-based rigid registration error was reduced 40% to 4.4 mm with nonrigid correction.

The tumor centroid distance continues to improve when including a subsurface feature near the tumor (*k*=1), improving 55% over point-based rigid registration as shown in Table 2. Table 1 shows the small detriment to surface alignment with a small improvement in subsurface alignment. In Table 1, subsurface error is still computed at all 14 subsurface features, though one of these features is considered a mock biopsy clip (and therefore added to the data driving model correction). If this driving feature point is excluded from the subsurface error computation, a true measurement of TRE, the subsurface registration error is 3.4 ± 1.0 mm (compared to 3.3 ± 1.1 mm as reported in Table 1).

Though not feasible in the operating room, including the full tumor surface provides a theoretical best-case scenario for the current modeling approach, while the iterative closest point registration offers a theoretical best-case scenario for tumor overlap with rigid registration. Although the rigid ICP approach outperforms model correction at the tumor, all nonrigid approaches outperform rigid alignment at fiducials and subsurface features.

5. CONCLUSION

This work presents a novel deformation correction approach in breast conserving surgery that achieves clinically relevant registration accuracy using realistically obtainable intraoperative data. Moreover, this demonstrates an initial investigation into the impact of providing subsurface features to a model to improve localization accuracy; including subsurface features in a modeling approach has the potential to offer even further improvement. This deformation correction framework has the potential to significantly improve intraoperative tumor localization in breast conserving surgery by better predicting image-to-surgery breast shape changes.

ACKNOWLEDGEMENTS

This work was supported by NIH-NIBIB awards T32EB021937, R21EB022380, R01EB027498, and Vanderbilt grant 1S10OD021771-01.

REFERENCES

[1] R. L. Siegel, K. D. Miller, H. E. Fuchs, and A. Jemal, "Cancer statistics, 2022," *CA: a cancer journal for clinicians,* 2022.

[2] M. Golshan, C. T. Cirrincione, W. M. Sikov, D. A. Berry, S. Jasinski, T. F. Weisberg, G. Somlo, C. Hudis, E. Winer, and D. W. Ollila, "Impact of neoadjuvant chemotherapy in stage II–III triple negative breast cancer on eligibility for breast-conserving surgery and breast conservation rates: surgical results from CALGB 40603 (Alliance)," *Annals of surgery,* vol. 262, no. 3, p. 434, 2015.

[3] A. A. H. Gladden, S. Sams, A. Gleisner, C. Finlayson, N. Kounalakis, P. Hosokawa, R. Brown, T. Chong, D. Mathes, and C. Murphy, "Re-excision rates after breast conserving surgery following the 2014 SSO-ASTRO guidelines," *The American Journal of Surgery,* vol. 214, no. 6, pp. 1104-1109, 2017.

[4] M. T. van Leeuwen, M. O. Falster, C. M. Vajdic, P. J. Crowe, S. Lujic, E. Klaes, L. Jorm, and A. Sedrakyan, "Reoperation after breast-conserving surgery for cancer in Australia: statewide cohort study of linked hospital data," *BMJ open,* vol. 8, no. 4, p. e020858, 2018.

[5] L. Hughes, J. Hamm, C. McGahan, and C. Baliski, "Surgeon volume, patient age, and tumor-related factors influence the need for re-excision after breast-conserving surgery," *Annals of Surgical Oncology,* vol. 23, no. 5, pp. 656-664, 2016.

[6] O. Kantor, C. Pesce, K. Kopkash, E. Barrera, D. J. Winchester, K. Kuchta, and K. Yao, "Impact of the Society of Surgical Oncology-American Society for Radiation Oncology margin guidelines on breast-conserving surgery and mastectomy trends," *Journal of the American College of Surgeons,* vol. 229, no. 1, pp. 104-114, 2019.

[7] P. Siegler, C. M. Holloway, P. Causer, G. Thevathasan, and D. B. Plewes, "Supine breast MRI," *J Magn Reson Imaging,* vol. 34, no. 5, pp. 1212-7, Nov 2011.

[8] R. M. Mann, C. K. Kuhl, and L. Moy, "Contrast-enhanced MRI for breast cancer screening," *Journal of Magnetic Resonance Imaging,* vol. 50, no. 2, pp. 377-390, 2019.

[9] B. K. Byrd, V. Krishnaswamy, J. Gui, T. Rooney, R. Zuurbier, K. Rosenkranz, K. Paulsen, and R. J. Barth, "The shape of breast cancer," *Breast Cancer Research and Treatment,* pp. 1-8, 2020.

[10] E. C. Gombos, J. Jayender, D. M. Richman, D. L. Caragacianu, M. A. Mallory, F. A. Jolesz, and M. Golshan, "Intraoperative supine breast MR imaging to quantify tumor deformation and detection of residual breast cancer: preliminary results," *Radiology,* vol. 281, no. 3, pp. 720-729, 2016.

[11] S. Joukainen, A. Masarwah, M. Könönen, M. Husso, A. Sutela, V. Kärjä, R. Vanninen, and M. Sudah, "Feasibility of mapping breast cancer with supine breast MRI in patients scheduled for oncoplastic surgery," *European Radiology,* Journal Article vol. 29, no. 3, pp. 1435-1443, August 17 2019.

[12] M. Sakakibara, T. Nagashima, T. Sangai, R. Nakamura, H. Fujimoto, M. Arai, T. Kazama, H. Hashimoto, Y. Nakatani, and M. Miyazaki, "Breast-Conserving Surgery Using Projection and Reproduction Techniques of Surgical-Position Breast MRI in Patients with Ductal Carcinoma In Situ of the Breast," *Journal of the American College of Surgeons,* vol. 207, no. 1, pp. 62-68, 2008/07/01/ 2008.

[13] R. J. Barth, V. Krishnaswamy, K. D. Paulsen, T. B. Rooney, W. A. Wells, C. V. Angeles, R. A. Zuurbier, K. Rosenkranz, S. Poplack, and T. D. Tosteson, "A Randomized Prospective Trial of Supine MRI-Guided Versus Wire-Localized Lumpectomy for Breast Cancer," *Annals of Surgical Oncology,* pp. 1-10, 2019.

[14] S. L. Perkins, M. A. Lin, S. Srinivasan, A. J. Wheeler, B. A. Hargreaves, and B. L. Daniel, "A mixed-reality system for breast surgical planning," in *2017 IEEE International Symposium on Mixed and Augmented Reality (ISMAR-Adjunct)*, 2017, pp. 269-274: IEEE.

[15] Z.-Y. Wu, H. J. Kim, J. Lee, I. Y. Chung, J. Kim, S. Lee, B. H. Son, S.-H. Ahn, H. H. Kim, and J. B. Seo, "Breast-conserving surgery with 3D-printed surgical guide: a single-center, prospective clinical study," *Scientific Reports,* vol. 11, no. 1, pp. 1-8, 2021.

[16] W. L. Richey, J. S. Heiselman, M. Luo, I. M. Meszoely, and M. I. Miga, "Impact of deformation on a supine-positioned image guided breast surgery approach," *International Journal of Computer Assisted Radiology and Surgery,* Journal vol. 16, no. 11, p. 2055—2066, 2021.

[17] M. Ebrahimi, P. Siegler, A. Modhafar, C. M. Holloway, D. B. Plewes, and A. L. Martel, "Using surface markers for MRI guided breast conserving surgery: a feasibility survey," *Phys Med Biol,* vol. 59, no. 7, pp. 1589-605, Apr 7 2014.

[18] R. H. Conley, I. M. Meszoely, J. A. Weis, T. S. Pheiffer, L. R. Arlinghaus, T. E. Yankeelov, and M. I. Miga, "Realization of a biomechanical model-assisted image guidance system for breast cancer surgery using supine MRI," (in English), *International Journal of Computer Assisted Radiology and Surgery,* Article vol. 10, no. 12, pp. 1985-1996, Dec 2015.

[19] J. S. Heiselman, W. R. Jarnagin, and M. I. Miga, "Intraoperative correction of liver deformation using sparse surface and vascular features via linearized iterative boundary reconstruction," *IEEE Transactions on Medical Imaging,* vol. 39, no. 6, pp. 2223-2234, 2020.

[20] J. M. Sullivan Jr, G. Charron, and K. D. Paulsen, "A three-dimensional mesh generator for arbitrary multiple material domains," *Finite Elements in Analysis and Design,* vol. 25, no. 3-4, pp. 219-241, 1997.

[21] M.-P. Dubuisson and A. K. Jain, "A modified Hausdorff distance for object matching," in *Proceedings of 12th international conference on pattern recognition*, 1994, vol. 1, pp. 566-568: IEEE.